

## Supporting Information

### Layered $\text{Bi}_2\text{Te}_3$ Nanoplates/Graphene Composites with High Gravimetric and Volumetric Performance for Na-Ion Storage

Dianding Sun,<sup>†,a</sup> Guanjun Zhang,<sup>†,a</sup> Dan Li,<sup>a</sup> Sitong Liu,<sup>a</sup> Xiaolong Jia<sup>\*,b,c</sup> and Jisheng Zhou<sup>\*,a</sup>

<sup>a</sup> State Key Laboratory of Chemical Resource Engineering, Beijing Key Laboratory of Electrochemical Process and Technology for Materials, Beijing University of Chemical Technology, Beijing, P. R. China.

<sup>b</sup> State Key Laboratory of Organic-Inorganic Composites, College of Materials Science and Engineering, Beijing University of Chemical Technology, Beijing, 100029, P. R. China

<sup>c</sup> Key Laboratory of Carbon Fiber and Functional Polymer, Ministry of Education, Beijing University of Chemical Technology, Beijing, 100029, P. R. China

<sup>†</sup> Authors with equal contributions

\* Corresponding authors: zhoujs@mail.buct.edu.cn (J Zhou); jiaxl@mail.buct.edu.cn (X. Jia)

#### Supporting Data:

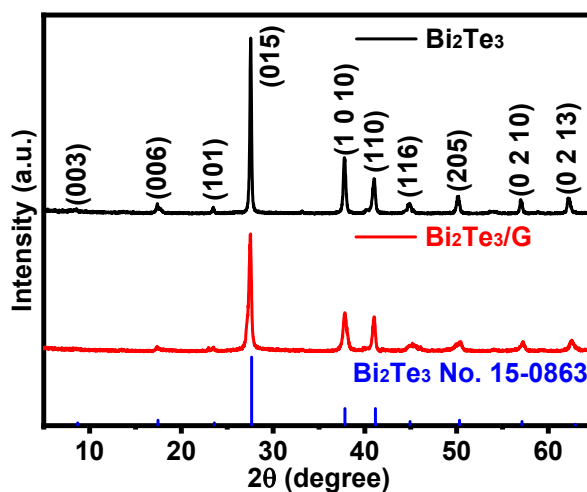
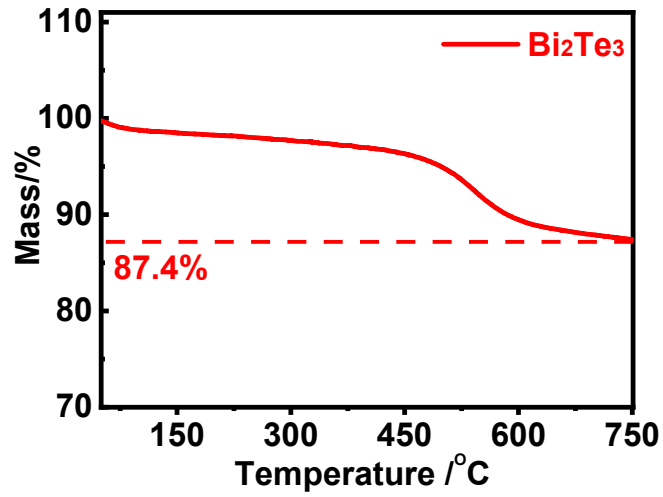
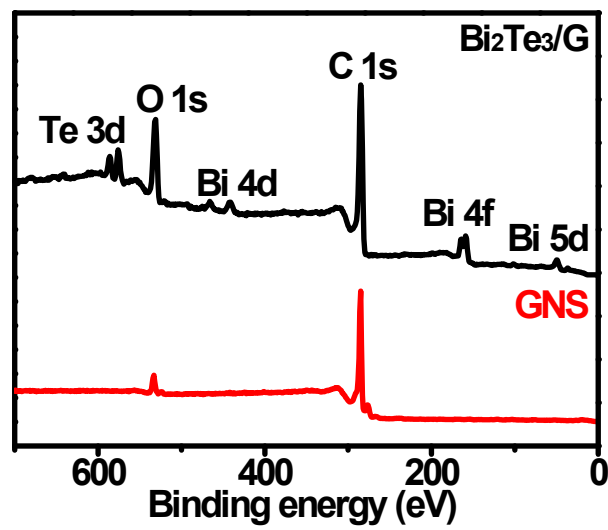


Fig. S1 XRD patterns of pure  $\text{Bi}_2\text{Te}_3$  and  $\text{Bi}_2\text{Te}_3/\text{G}$  composite.



**Fig. S2** TG curve of  $\text{Bi}_2\text{Te}_3/\text{G}$  composite obtained in air atmosphere from room temperature to 800  $^\circ\text{C}$  at a rate of 10  $^\circ\text{C min}^{-1}$ .



**Fig. S3** XPS survey spectra of the  $\text{Bi}_2\text{Te}_3/\text{G}$  composite and GNS.

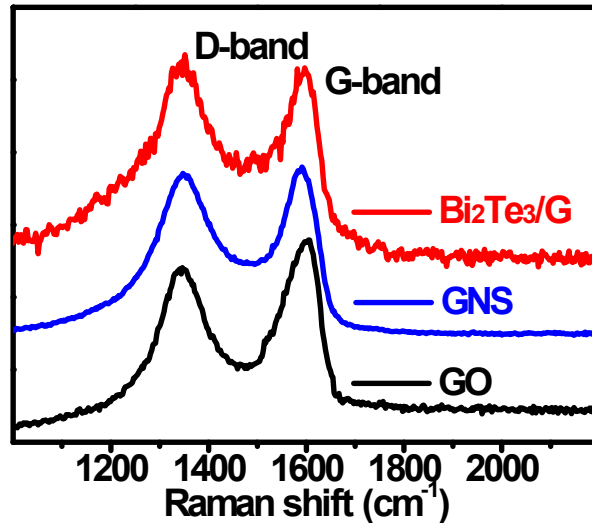


**Fig. S4** Raman spectra of GO, GNS, and  $\text{Bi}_2\text{Te}_3/\text{G}$  composite.

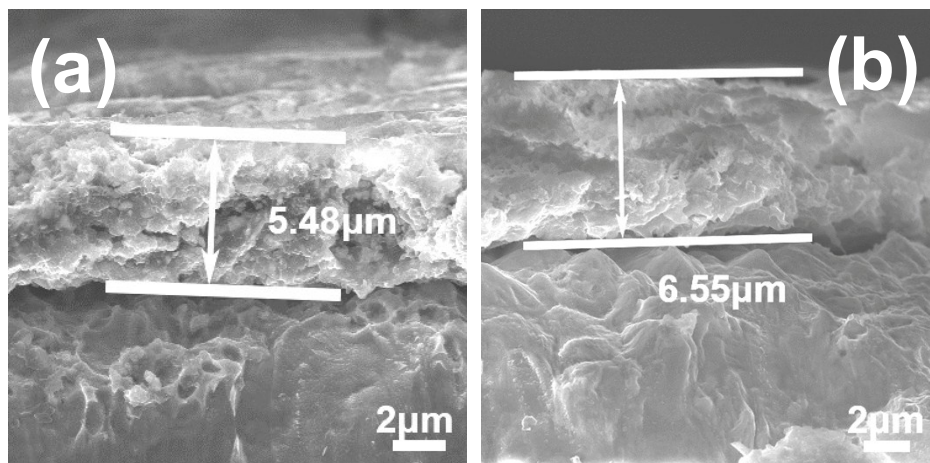


**Fig. S5** Cross-section SEM images of (a) fresh  $\text{Bi}_2\text{Te}_3/\text{G}$  electrode with mass loading of 1.31 mg and (b) the  $\text{Bi}_2\text{Te}_3/\text{G}$  electrode after 50 cycles at  $1 \text{ A g}^{-1}$  with mass loading: 1.43 mg.

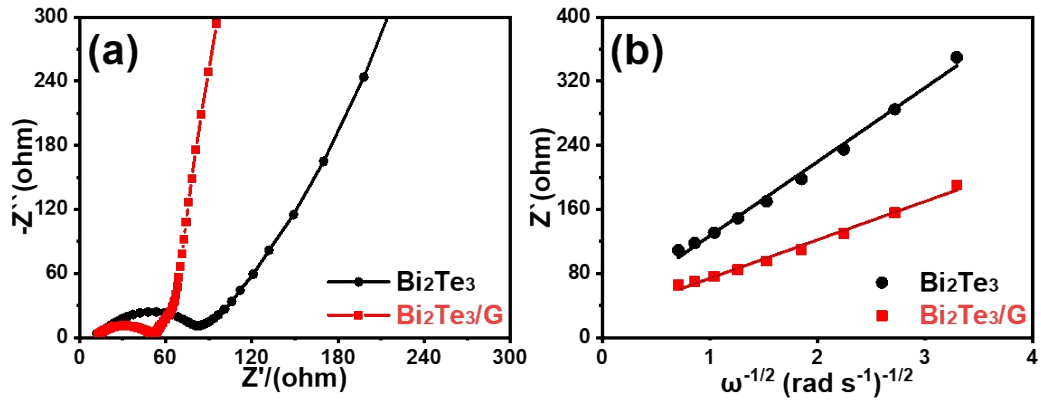


**Fig. S6** (a) EIS curves of pure  $\text{Bi}_2\text{Te}_3$  and  $\text{Bi}_2\text{Te}_3/\text{G}$  composite obtained after two cycles at  $1 \text{ A g}^{-1}$ ; and (b) the relationship plots between  $Z'$  and  $\omega^{-1/2}$  at low-frequency region of pure  $\text{Bi}_2\text{Te}_3$  and  $\text{Bi}_2\text{Te}_3/\text{G}$  composite.

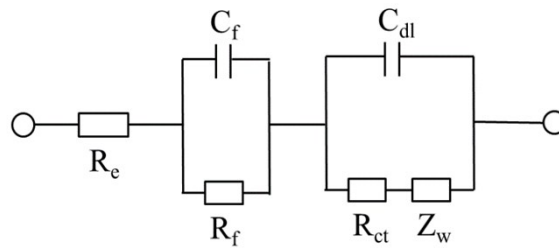


**Fig. S7** Equivalent circuit used for fitting of EIS curves (Fig. S5), where  $R_e$  is the electrolyte resistance;  $C_f$  and  $R_f$  are the capacitance and resistance of the surface SEI film formed on the electrodes, respectively;  $C_{dl}$  and  $R_{ct}$  are the double-layer capacitance and charge-transfer resistance, respectively;  $Z_w$  is the Warburg impedance related to the diffusion of Na-ions into the bulk electrodes.

**Table S1** Layered chalcogenide and their corresponding interlayer spacing.

Materials	Interlayer Spacing (Å)	Materials	Interlayer Spacing (Å)	Materials	Interlayer Spacing (Å)
Bi <sub>2</sub> Se <sub>3</sub>	9.56	PdTe <sub>2</sub>	5.13	TiS <sub>2</sub>	5.70
<b>Bi<sub>2</sub>Te<sub>3</sub></b>	<b>10.16</b>	PtS <sub>2</sub>	5.02	TiSe <sub>2</sub>	5.99
CoTe <sub>2</sub>	5.40	PtSe <sub>2</sub>	5.06	TiTe <sub>2</sub>	6.51
GaTe <sub>3</sub>	5.90	PtTe <sub>2</sub>	5.20	VS <sub>2</sub>	5.73
HfS <sub>2</sub>	5.84	ReS <sub>2</sub>	6.08	WS <sub>2</sub>	6.18
HfSe <sub>2</sub>	6.16	RhTe <sub>2</sub>	5.41	WSe <sub>2</sub>	6.49
IrTe <sub>2</sub>	5.39	Si <sub>2</sub> Te <sub>3</sub>	6.74	WTe <sub>2</sub>	7.02
MoS <sub>2</sub>	6.20	SiTe <sub>2</sub>	6.71	ZrS <sub>2</sub>	5.81
MoSe <sub>2</sub>	6.50	SnS <sub>2</sub>	5.87	ZrSe <sub>2</sub>	6.14
MoTe <sub>2</sub>	7.00	SnSe <sub>2</sub>	6.14	ZrSe <sub>3</sub>	9.36
NbS <sub>2</sub>	5.96	SnSSe	6.05	ZrTe <sub>2</sub>	6.63
NiTe <sub>2</sub>	5.30	TaS <sub>2</sub>	5.86	ZrTe <sub>3</sub>	10.01

**Table S2** Electrochemical performance comparison of some advanced metal telluride anode materials for SIBs.

Materials	Voltage range (V)	Initial Coulombic efficiency (%)	Initial discharge/charge Capacity (mAh/g)	Rate performance			Cycle life	Ref.
				Gravimetric capacity (mAh/g)	Volumetric capacity (mAh/cm <sup>3</sup> )	Current rate (A/g)		
FeTe <sub>2</sub> -rGO	0.001-3.0	76	493/373	421	---	0.1	80	1
				384	---	0.5		
				362	---	1		
				321	---	2		
				257	---	3		
C@MoTe <sub>2</sub>	0.001-3.0	71.9	388/279	343	---	0.2	200	2
				306	---	0.5		
				280	---	1		
				254	---	2		
				236	---	3		
SnTe/C	0.001-2.5	62.7	541/339	209	---	5	100	3
				316	639	0.03		
				292	600	0.06		
				272	540	0.16		
				243	490	0.32		
C@Cu <sub>1.75</sub> Te	0.005-3.0	37.3	843/314	225	455	0.64	500	4
				213	430	0.96		
				245.2	---	0.2		
				127.8	---	0.5		
				68.1	---	1		
NiTe <sub>2</sub> @NCNs	0.3-2.8	94.1	284.5/267.7	44.4	---	3	5000	5
				289.5	---	0.1		
				281.5	---	1		
				275.7	---	2		
				271.6	---	5		
Bi <sub>2</sub> Te <sub>3</sub>	0.3-2.8	79.3	464/368	247.3	910.0	0.1	50	This work
				183.5	675.2	0.2		
				98.4	362.1	0.5		
				50.4	185.4	1.0		
				26.4	97.1	2.0		
Bi <sub>2</sub> Te <sub>3</sub> /G	0.3-2.8	83.5	498/416	11.7	43.0	5.0	500	This work
				312.9	488.1	0.1		
				302.9	472.5	0.2		
				275.2	429.3	0.5		
				252.2	393.4	1.0		
				229.2	357.6	2.0		
				203.1	316.8	5.0		

**Table S3** Fitting results of the EIS curves for the pure Bi<sub>2</sub>Te<sub>3</sub> and Bi<sub>2</sub>Te<sub>3</sub>/G composite.

Samples	R <sub>e</sub> (Ω)	R <sub>f</sub> (Ω)	R <sub>ct</sub> (Ω)	σ (Ω rad <sup>1/2</sup> s <sup>-1/2</sup> )	D (cm <sup>2</sup> S <sup>-1</sup> )
Bi <sub>2</sub> Te <sub>3</sub>	14.3	12.5	49.10	93.59	2.36E-18
Bi <sub>2</sub> Te <sub>3</sub> /G	13.21	12.64	18.22	48.07	1.45E-16

## References

- 1 J. S. Cho, S. Y. Lee, J.-K. Lee and Y.C. Kang, *Acs Appl.Mater.Interfaces*, 2016, **8**, 21343-21349.
- 2 J. S. Cho, H. S. Ju, J.-K. Lee and Y. C. Kang, *Nanoscale*, 2017, **9**, 1942-1950.

- 3 A.-R. Park and C.-M. Park, *ACS Nano*, 2017, **5**, 5884-5901.
- 4 H. Yu, J. Yang, H. Geng and C. Li, *Nanotechnology*, 2017, **28**, 145403.
- 5 D. Sun, S. Liu, G. Zhang and J. Zhou, *Chem. Eng. J.*, 2019, **359**, 1659-1667.